INORGANIC CHEMISTRY FRONTIERS

RESEARCH ARTICLE

View Article Online
View Journal | View Issue

Cite this: *Inorg. Chem. Front.*, 2022, **9**, 2264

An unprecedented C_{80} cage that violates the isolated pentagon rule†

Pengwei Yu,‡[a] Mengyang Li,‡[b] Wangqiang Shen,[a] Shuaifeng Hu,[a] Peng-Yuan Yu,[a] Xinyue Tian,[a] Xiang Zhao, *[b] Lipiao Bao *[a] and Xing Lu *[a]

Received 23rd February 2022,
Accepted 25th March 2022

DOI: 10.1039/d2qi00410k

rsc.li/frontiers-inorganic

Two $Lu_2O@C_{80}$ isomers have been successfully isolated and unambiguously assigned as $Lu_2O@C_1(31876)$-C_{80} and $Lu_2O@C_{2v}(5)$-C_{80}, respectively, by X-ray crystallography. Interestingly, $C_1(31876)$-C_{80} is an unprecedented cage with a pair of adjacent pentagons, which can be closely connected with $C_{2v}(5)$-C_{80} *via* a two-step Stone–Wales transformation. More importantly, the $C_1(31876)$-C_{80} cage is a key point in the transformation map of oxide cluster fullerenes, filling the vacancy in the formation process.

Introduction

Endohedral metallofullerenes (EMFs) are a collection of novel molecules formed by the encapsulation of metal ions or clusters in fullerene cages.[1,2] One of the most prominent features of these compounds is the charge transfer from the inner metallic species to the outer cages, thus stabilizing many cages that are unstable as empty fullerenes.[3] For example, $D_{5d}(1)$-C_{80} and $D_2(2)$-C_{80} were separated as empty cages, but the encapsulation of M_3N clusters accompanied by 6-electron transfer (M = Lu, Dy) promoted the formation of $D_{5h}(6)$-C_{80} and $I_h(7)$-C_{80}.[4–8] In particular, the pristine cages of metallofullerenes can violate the isolated pentagon rule (IPR) that all empty fullerenes must obey because local steric strain on the adjacent pentagons (pentalene unit) can be released through interaction with the encapsulated metal.[9–12] Since the first isolation of $Sc_2@C_{2v}(4348)$-C_{66} and $Sc_3N@D_3(6140)$-C_{68} in 2000, endohedrals that do not obey the IPR have received wide attention due to their unusual structures.[13,14]

The formation mechanism of fullerenes remains unclear and controversial because their formation process cannot yet be directly observed. Fortunately, comprehensive inter-cage transformation pathways with cages containing pentalene units as key points are conducive to understanding the rearrangement process of fullerenes.[15] Dorn *et al.* have shown that the unique asymmetric cage of $M_2C_2@C_1(51383)$-C_{84} (M = Y, Gd) is a "missing link" in well-established conversion pathways to form many high-symmetry fullerene cages, which provides structural evidence for the top-down mechanism.[16] Meanwhile, the bottom-up mechanism has also been well developed; Echegoyen *et al.* suggested that the nonclassical $Sc_2C_2@C_s(hept)$-C_{88} with a heptagon could be obtained from $Sc_2C_2@C_{2v}(9)$-C_{86} through a simple C_2 insertion.[17] Recently, the interconversions between all isolated uranium-based mono-metallofullerenes reported by Chen *et al.* demonstrated that some cages with a pentalene unit can serve as precursors to form larger or smaller cages, indicating the simultaneous top-down and bottom-up processes.[18,19] Accordingly, disclosing new cages that violate the isolated pentagon rule is crucial for completing the transformation map and revealing the formation mechanism of fullerenes.

Herein, we report the synthesis and isolation of two C_{80} isomers containing a Lu_2O cluster. X-ray crystallographic results unambiguously reveal their molecular structures as $Lu_2O@C_1(31876)$-C_{80} and $Lu_2O@C_{2v}(5)$-C_{80}, respectively. It is rather surprising that a $Lu_2O@C_1(31876)$-C_{80} isomer with a pair of adjacent pentagons has a relatively high yield, and its cage can be interconverted to the $C_{2v}(5)$-C_{80} cage through a two-step Stone–Wales transformation. Importantly, with the discovery of the unique $C_1(31876)$-C_{80}, a transformation map including the major cages of the reported dimetallic oxide cluster fullerenes is completed.

Results and discussion

Lutetium-based metallofullerenes were synthesized in an arc-discharge reactor under a He/CO_2 atmosphere (270/15 Torr).[20]

[a]*State Key Laboratory of Materials Processing and Die & Mould Technology, School of Materials Science and Engineering, Huazhong University of Science and Technology, 1037 Luoyu Road, Wuhan, 430074 China. E-mail: baol@hust.edu.cn, lux@hust.edu.cn*

[b]*Institute of Molecular Science & Applied Chemistry, School of Chemistry, Xi'an Jiaotong University, Xi'an 710049, China. E-mail: xzhao@mail.xjtu.edu.cn*

†Electronic supplementary information (ESI) available. CCDC 2131027 and 2131029. For ESI and crystallographic data in CIF or other electronic format see DOI: https://doi.org/10.1039/d2qi00410k

‡These authors contributed equally.

After ultrasonic extraction in carbon disulfide (CS_2), multistage high-performance liquid chromatography (HPLC) separation gave pure $Lu_2O@C_1(31876)$-C_{80} and $Lu_2O@C_{2v}(5)$-C_{80} samples (Fig. S1†). The analytical HPLC chromatograms and the laser-desorption ionization time-of-flight (LDI-TOF) mass spectra confirmed their high purity (Fig. S2†).

Absorption measurements were carried out for the two $Lu_2O@C_{80}$ isomers (Fig. 1a), which present obviously different characteristic absorptions in CS_2. In detail, the $Lu_2O@C_1(31876)$-C_{80} isomer shows seven absorption peaks at 531, 592, 640, 834, 882, 940, and 1376 nm, whereas for $Lu_2O@C_{2v}(5)$-C_{80}, six absorption peaks at 470, 618, 651, 688, 834, and 1399 nm are observed. Meanwhile, the absorption onsets of $Lu_2O@C_1(31876)$-C_{80} and $Lu_2O@C_{2v}(5)$-C_{80} are around 1459 and 1600 nm, corresponding to small optical band gaps of 0.85 and 0.78 eV, respectively. The absorption features of $Lu_2O@C_{2v}(5)$-C_{80} resemble those of $Sc_2O@C_{2v}(5)$-C_{80} [21] and $Sc_2C_2@C_{2v}(5)$-C_{80},[22] indicating a four-electron transfer from the Lu_2O cluster to the cage.

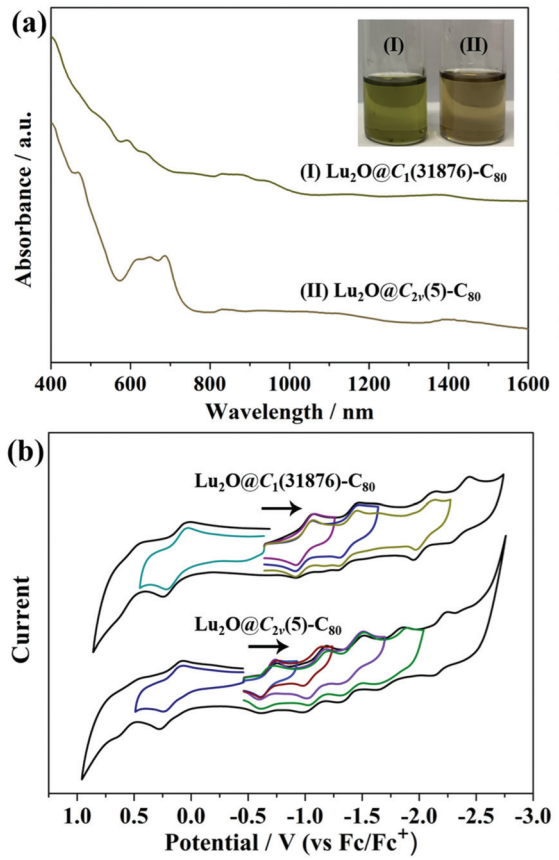

Fig. 1 (a) Vis-NIR absorption spectra of (I) $Lu_2O@C_1(31876)$-C_{80} and (II) $Lu_2O@C_{2v}(5)$-C_{80} in CS_2 at room temperature (concentration: 0.2 mg mL^{-1}). Inset: Photograph of the corresponding sample solutions. (b) Cyclic voltammograms of $Lu_2O@C_1(31876)$-C_{80} and $Lu_2O@C_{2v}(5)$-C_{80} in 0.05 M $TBAPF_6$/*o*-DCB solution (scan direction: negative; scan rate: 100 mV s^{-1}).

The electrochemical properties of the $Lu_2O@C_{80}$ isomers were studied by cyclic voltammetry (Fig. 1b) and their redox potentials are summarized in Table 1 along with those of $Sc_2O@C_{2v}(5)$-C_{80}. In the anodic region, both $Lu_2O@C_{80}$ isomers exhibit two fully reversible oxidation processes. The first and second oxidation potentials of $Lu_2O@C_1(31876)$-C_{80} are very close to the corresponding potentials of $Lu_2O@C_{2v}(5)$-C_{80}. On the other hand, in the cathodic region, four and five reversible reduction processes are observed for $Lu_2O@C_1(31876)$-C_{80} and $Lu_2O@C_{2v}(5)$-C_{80}, respectively. The first reduction potential of $Lu_2O@C_1(31876)$-C_{80} shifts by −240 mV relative to that of $Lu_2O@C_{2v}(5)$-C_{80}. Consequently, the electrochemical gap of $Lu_2O@C_1(31876)$-C_{80} (1.14 V) is larger than that of $Lu_2O@C_{2v}(5)$-C_{80} (0.95 V), which is in line with the absorption results. These results indicate that the difference in the cage structure has a considerable effect on the electrochemical behavior of the two molecules, especially on their lowest unoccupied molecular orbital energy, which is also reflected in the frontier molecular orbital analysis (Fig. S5†). Moreover, the redox behavior of $Lu_2O@C_{2v}(5)$-C_{80} resembles that of $Sc_2O@C_{2v}(5)$-C_{80},[21] indicating their similar electronic structure. Thus, it can be concluded that the outer cage structure instead of the metallic unit has important influences on the electrochemical behavior of dimetallic oxide cluster fullerenes.

High-quality co-crystals of the two $Lu_2O@C_{80}$ isomers and Ni^{II}(OEP) (OEP = 2,3,7,8,12,13,17,18-octaethylporphin dianion) were obtained by layering a benzene solution of Ni^{II}(OEP) over a CS_2 solution of each endohedral. Their molecular structures were unambiguously determined by single-crystal X-ray diffraction (XRD) crystallography as $Lu_2O@C_1(31876)$-C_{80} and $Lu_2O@C_{2v}(5)$-C_{80}, respectively. In particular, this is the first identification of the $C_1(31876)$-C_{80} cage, which contains a pair of adjacent pentagons. The details of the crystallographic data are listed in Table S1.† The refined structures of $Lu_2O@C_1(31876)$-C_{80}·Ni^{II}(OEP) and $Lu_2O@C_{2v}(5)$-C_{80}·Ni^{II}(OEP) with the major metal sites are shown in Fig. 2. The porphyrin moiety leans towards the relatively flat region of each fullerene cage with the shortest Ni-to-cage-carbon distance of 2.959 Å

Table 1 Redox potentials (*V vs.* Fc/Fc^+) and electrochemical bandgaps of $Lu_2O@C_1(31876)$-C_{80}, $Lu_2O@C_{2v}(5)$-C_{80} and $Sc_2O@C_{2v}(5)$-C_{80}

Species	$^{ox}E_2$	$^{ox}E_1$	$^{red}E_1$	$^{red}E_2$	$^{red}E_3$	$^{red}E_4$	$^{red}E_5$	ΔE_{gap} [c]	Ref.
$Lu_2O@C_1(31876)$-C_{80}	0.53[a]	0.15[a]	−0.99[a]	−1.38[a]	−2.05[a]	−2.36[a]		1.14	This work
$Lu_2O@C_{2v}(5)$-C_{80}	0.56[a]	0.20[a]	−0.75[a]	−1.12[a]	−1.44[a]	−1.78[a]	−2.19[a]	0.95	This work
$Sc_2O@C_{2v}(5)$-C_{80}	0.56[a]	0.24[a]	−0.89[b]	−1.48[b]	−1.75[b]	−1.96[b]	−2.13[b]	1.13	20

[a] Half-wave potential in volts (reversible redox process). [b] Peak potential in volts (irreversible redox process). [c] $\Delta E_{gap} = {}^{ox}E_1 - {}^{red}E_1$.

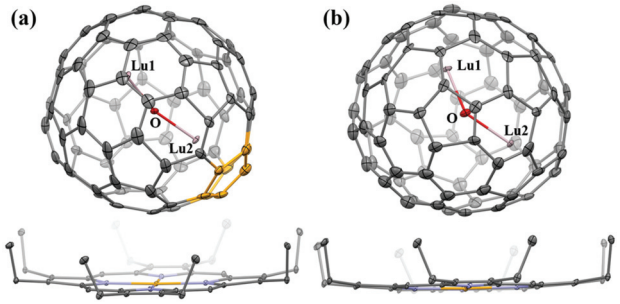

Fig. 2 ORTEP drawings of (a) $Lu_2O@C_1(31876)$-C_{80}·Ni^{II}(OEP) and (b) $Lu_2O@C_{2v}(5)$-C_{80}·Ni^{II}(OEP). Thermal contours are drawn at the 10% probability level. Only one fullerene cage and the predominant metal sites are shown, whereas minor metal sites, solvent molecules and H atoms are omitted for clarity.

and 2.899 Å for $Lu_2O@C_1(31876)$-C_{80} and $Lu_2O@C_{2v}(5)$-C_{80}, respectively, indicating substantial π–π interactions between the cluster fullerenes and Ni^{II}(OEP) molecules.[23] Inside the two fullerene cages, the central oxygen atoms are both fully ordered, but the Lu atoms exhibit a certain degree of disorder (Fig. S3 and Table S2†), implying the motional behavior of the Lu atoms. Interestingly, it was found that one Lu atom prefers to vibrate near the adjacent pentagons in $Lu_2O@C_1(31876)$-C_{80}, which is similar to the motion of metal atoms in the IPR-violating $Dy_2O@C_2(13333)$-C_{74}.[24] This phenomenon implies that the stabilization of cages that violate the isolated pentagon rule requires sufficient metal–pentalene coordination interactions.[25] For the major metal sites (Fig. S4 and Table S3†), the average distance between Lu2 and the pentalene motif in $Lu_2O@C_1(31876)$-C_{80} is 2.389 Å, shorter than the other metal–cage distances inside the two isomers (2.570 Å for Lu1 in $Lu_2O@C_1(31876)$-C_{80}; 2.526 Å for Lu1 and 2.581 Å for Lu2 in $Lu_2O@C_{2v}(5)$-C_{80}). The Lu1–O–Lu2 angle in $Lu_2O@C_1(31876)$-C_{80} is 157.05°, larger than the value observed in $Lu_2O@C_{2v}(5)$-C_{80} (141.80°). These phenomena suggest that the pentalene unit in $Lu_2O@C_1(31876)$-C_{80} could provide stronger metal–pentalene interactions and extra space through protruding the cage.[26]

A complete transformation map of fullerenes can provide reliable evidence for understanding the formation mechanism. Importantly, the unique $C_1(31876)$-C_{80} cage under study is essential to complete a transformation map for the major cages of the reported dimetallic oxide cluster fullerenes. The transformation processes involving $C_1(31876)$-C_{80} simply require at most two well-established steps, *i.e.*, the Stone–Wales transformation (SWT) or C_2 loss.[27,28] Fig. 3 depicts the

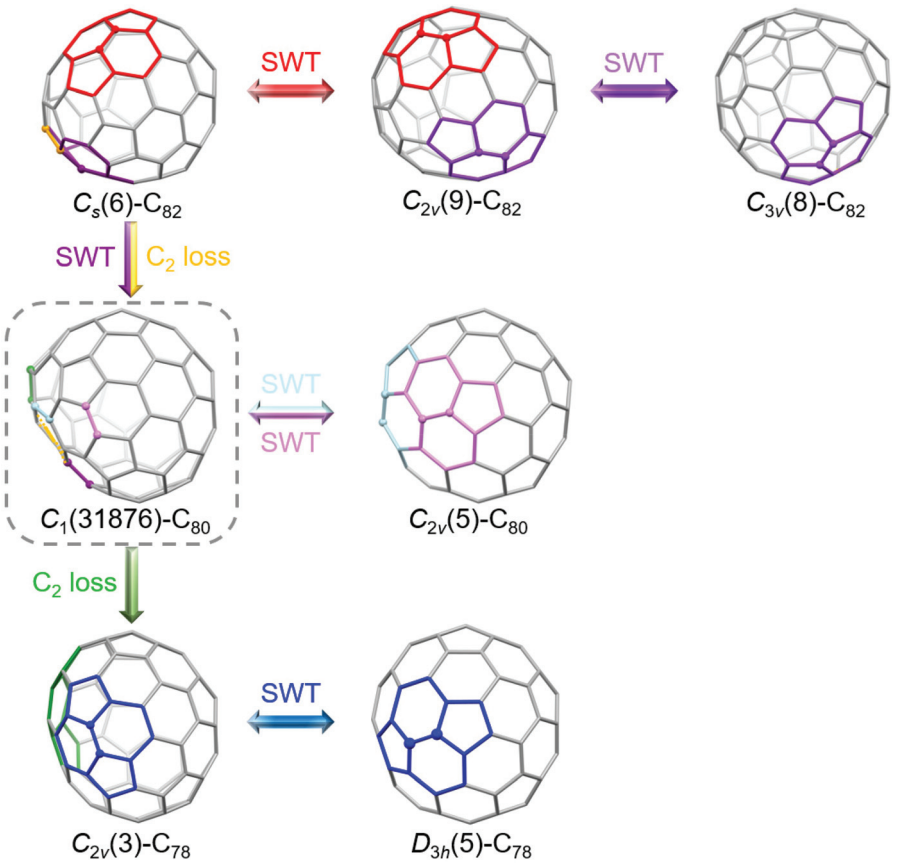

Fig. 3 Fullerene transformation map related to the $C_1(31876)$-C_{80} cage. Colors are used to visualize the motifs involved in the steps indicated by matching colored arrows.

transformation map related to the C_1(31876)-C_{80} cage and the detailed path of each step is illustrated in the ESI (Fig. S6–S10†). Structural rearrangements are demonstrated among three isomeric C_{82} cages, namely C_s(6)-C_{82}, C_{2v}(9)-C_{82} and C_{3v}(8)-C_{82}, *via* merely one SWT. C_1(31876)-C_{80} is obtainable through a C_2-unit loss in the pentalene motif generated by a SWT on C_s(6)-C_{82}. Then two successive SWTs on C_1(31876)-C_{80} afford C_{2v}(5)-C_{80}. In addition, the transformation from C_1(31876)-C_{80} to C_{2v}(3)-C_{78} is straightforward *via* a C_2-unit loss on the pentalene motif, and then a further SWT on C_{2v}(3)-C_{78} produces D_{3h}(5)-C_{78}. Interestingly, it is evident that the formation process of dimetallic oxide cluster fullerenes is different from that of well-studied monometallic actinide metallofullerenes, in which IPR-violating C_1(17418)-C_{76} and C_1(28324)-C_{80} cages are considered as the key intermediates.[19,29] Thus, the present results also corroborate that endohedral metallic species affect the choice of the transformation pathways.[16]

Theoretical calculations were performed at the PBE/6-31G (d)~SDD level to investigate the origin of stability of the two $Lu_2O@C_{80}$ isomers. Fig. 4a and Table S4† show the relative energy and the energy gaps between the highest occupied molecular orbital (HOMO) and the lowest unoccupied molecular orbital (LUMO) of $Lu_2O@C_{80}$ isomers. Although $Lu_2O@I_h$(7)-C_{80} and $Lu_2O@D_{5h}$(6)-C_{80} possess the lowest energy of 0.0 and 3.4 kcal mol^{-1}, respectively, their HOMO–LUMO gaps are too small (0.13 eV and 0.20 eV for $Lu_2O@I_h$(7)-C_{80} and $Lu_2O@D_{5h}$(6)-C_{80}, respectively), which means that the electrons on the HOMOs of $Lu_2O@I_h$(7)-C_{80} and $Lu_2O@D_{5h}$(6)-C_{80} are easily excited, and thus these two isomers show high reactivity. On the basis of relative energy, $Lu_2O@C_1$(31876)-C_{80} and $Lu_2O@C_{2v}$(5)-C_{80} are thermodynamic candidates with large HOMO–LUMO gaps. To verify this prediction, statistic thermodynamic analysis (Fig. 4b) considering the entropy–enthalpy effect, which has been verified as an effective method to determine the stable isomers of metallofullerenes in theory, such as dimetallic oxide cluster fullerene $Sc_2O@C_{78}$,[30,31] was carried out. It is noteworthy that fullerenes are formed at very high temperatures (1500–3000 K) in an arc-discharge chamber. As shown in Fig. 4b, except for the highly reactive $Lu_2O@I_h$(7)-C_{80} and $Lu_2O@D_{5h}$(6)-C_{80} isomers, the two $Lu_2O@C_{80}$ isomers under study, namely $Lu_2O@C_1$(31876)-C_{80} and $Lu_2O@C_{2v}$(5)-C_{80}, are the dominant species at 1500–3000 K. Consequently, the more competitive $Lu_2O@C_1$(31876)-C_{80} and $Lu_2O@C_{2v}$(5)-C_{80} are obtained in the experiment instead of other isomers.

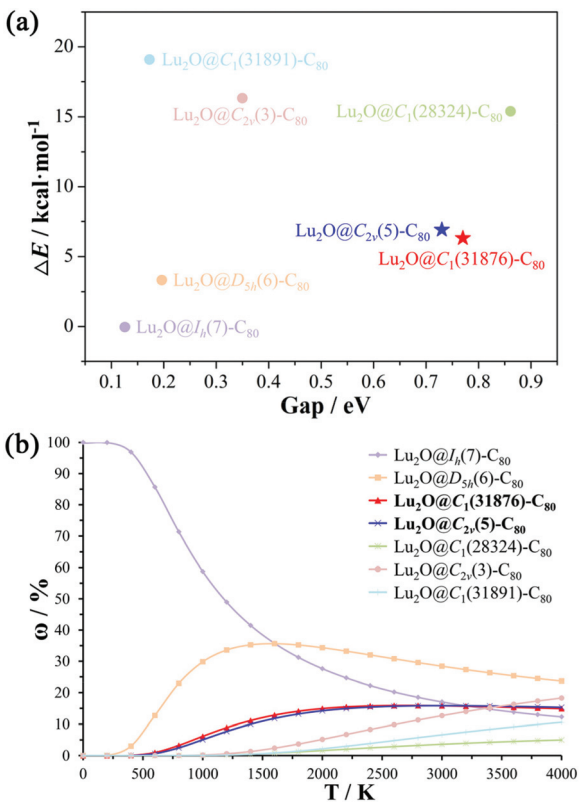

Fig. 4 (a) Relative energy (ΔE/kcal mol^{-1}) and the energy gaps (Gap/eV) between the HOMO and the LUMO, and (b) relative concentration (ω/%) at different temperatures (T/K) of $Lu_2O@C_{80}$ isomers on the PBE/6-31G (d)-SDD. Isomers are numbered according to the spiral algorithm of Fowler and Manolopoulos.[8] The simplified number is used for the IPR isomers.

Conclusions

In summary, two isomers of $Lu_2O@C_{80}$, namely $Lu_2O@C_1$(31876)-C_{80} and $Lu_2O@C_{2v}$(5)-C_{80}, have been successfully isolated and fully characterized by mass spectrometry, Vis-NIR absorption spectroscopy, cyclic voltammetry, single-crystal X-ray diffraction, and density functional theory calculations. Notably, this is the first observation of the C_1(31876)-C_{80} fullerene cage, which contains a pair of adjacent pentagons. Further structural study reveals that the C_1(31876)-C_{80} cage can serve as a key point in the transformation map for dimetallic oxide cluster fullerenes, filling the gap in the existing interconversion process. The current work demonstrates that the unique cage with adjacent pentagons may play a key role in the understanding of the long-standing puzzle about the formation mechanism and stimulates further interest in the exploration of more intermediates in the formation process.

Experimental

Materials

Lutetium(III) oxide (Lu_2O_3, 99.999%) was purchased from Suzhou Lanxi New Material Co., Ltd. Graphite rods (Ø 8 × 115 mm, 99.999%) and graphite powder (320 mesh, 99.999%) were purchased from Shanghai Fengyi Carbon Co., Ltd. Carbon disulfide (CS_2, 99.9%) was purchased from Aladdin company. Toluene (99.5%) was purchased from Sinopharm Chemical Reagent Co., Ltd. Chemicals were used as-received if not stated otherwise.

Preparation and isolation

A core-drilled graphite rod (6.88 g) was filled with a homogeneous mixture of Lu_2O_3 (4.26 g) and graphite powder (2.19 g). The rods were annealed in a tube furnace at 1000 °C for 12 hours under an argon atmosphere and then vaporized in a Krätschmer–Huffman-type fullerene generator with an arc current of 100 A under a mixture atmosphere of 270 Torr helium and 15 Torr CO_2. The as-produced fullerene soot was collected and sonicated in carbon disulfide for 1 h. After filtration, CS_2 was removed using a rotary evaporator. The solid residue was dissolved in toluene and filtered. The isolation of Lu-based metallofullerenes was achieved by a multiple-stage HPLC process conducted on an LC-918 machine (Japan Analytical Industry Co. Ltd). In these processes, a Buckyprep column (∅ 20 × 250 mm), a Buckyprep-M column (∅ 20 × 250 mm), and a 5PBB column (∅ 20 × 250 mm) (all Cosmosil, Nacalai Tesque, Japan) were used. More details about the HPLC processes are described in the ESI.† In this study, 300 rods were used to obtain the desired amount of the two metallofullerene samples.

Spectroscopic and electrochemical studies

LDI-TOF mass spectrometry was performed on a BIFLEX III spectrometer (Bruker Daltonics Inc., Germany). Vis-NIR spectra were obtained from a Lambda 35 spectrophotometer (PerkinElmer, USA) in CS_2. CV curves were obtained in *o*-dichlorobenzene with 0.05 M $TBAPF_6$ as the electrolyte using a CHI-660E instrument.

Crystallographic characterization

Black co-crystals of the metallofullerenes and Ni^{II}(OEP) were obtained by layering a benzene solution of Ni^{II}(OEP) over a CS_2 solution of the respective endohedrals in a glass tube at 0 °C for 30 days. Single-crystal X-ray data were collected at 100 K using a radiation wavelength of 0.73360 Å with a MarCCD detector at beamline BL17B in the Shanghai Synchrotron Radiation Facility. A multi-scan method was used for absorption corrections. The structures were solved by direct methods and refined with SHELXL-2014.[32] Hydrogen atoms were inserted at the calculated positions and constrained with isotropic thermal parameters. The details of crystal data are listed in the ESI.†

Computational studies

The optimizations of $Lu_2O@C_{80}$ isomers were carried out at the PBE/6-31G(d)~SDD level without any imaginary frequency,[33–36] where 6-31G(d) was for carbon and oxygen atoms and SDD with pseudopotentials was for lutetium atoms. PBE has been previously proved as a suitable functional for lutetium-based metallofullerenes.[37] Statistic thermodynamic analysis including the entropy–enthalpy effect was carried out to determine the thermodynamically stable $Lu_2O@C_{80}$ isomers based on PBE/6-31G(d)~SDD. Furthermore, single point calculations were conducted for thermodynamically stable $Lu_2O@C_{80}$ isomers on PBE/6-311G(d,p)~def2TZVP, where 6-311G(d,p) was for carbon and oxygen atoms and the def2TZVP basis set with a small-core relativistic pseudopotential (14s13p10d8f6g)/[6s6p5d4f3g] was for lutetium atoms.[38–41] All of the above calculations were performed with Gaussian 16 software except for the specific illustration.[42]

Author contributions

X. Lu, L. Bao and P. Yu designed the research. P. Yu carried out the experiments. M. Li carried out the calculations. P. Yu, M. Li, S. Hu, P.-Y. Yu, X. Tian and W. Shen carried out the analysis. X. Lu and X. Zhao supervised the project. P. Yu and M. Li co-wrote the paper. X. Lu, L. Bao and X. Zhao guided and revised the paper. All authors read and commented on the manuscript.

Conflicts of interest

There are no conflicts to declare.

Acknowledgements

Financial support from NSFC (No. 21925104, 21573172, and 21773181) and the Hubei Provincial Natural Science Foundation of China (No. 2021CFA020) is gratefully acknowledged. We thank the staff at the BL17B beamline of the National Center for Protein Sciences Shanghai (NCPSS) at Shanghai Synchrotron Radiation Facility for the assistance with data collection. We thank the Analytical and Testing Center in Huazhong University of Science and Technology for all related measurements. X. Z. acknowledges financial support from the Nanotechnology Platform Program (Molecule and Material Synthesis) of the Ministry of Education, Culture, Sports, Science, and Technology of Japan.

References

1 S. Yang, T. Wei and F. Jin, When metal clusters meet carbon cages: endohedral clusterfullerenes, *Chem. Soc. Rev.*, 2017, **46**, 5005–5058.
2 W. Shen, S. Hu and X. Lu, Endohedral Metallofullerenes: New Structures and Unseen Phenomena, *Chem. – Eur. J.*, 2020, **26**, 5748–5757.
3 R. Guan, M. Chen, F. Jin and S. Yang, Strain Release of Fused Pentagons in Fullerene Cages by Chemical Functionalization, *Angew. Chem., Int. Ed.*, 2020, **59**, 1048–1073.
4 F. H. Hennrich, R. H. Michel, A. Fischer, S. Richard-Schneider, S. Gilb, M. M. Kappes, D. Fuchs, M. Bürk, K. Kobayashi and S. Nagase, Isolation and Characterization of C_{80}, *Angew. Chem., Int. Ed. Engl.*, 1996, **35**, 1732–1734.
5 C. Wang, T. Sugai, T. Kai, T. Tomiyama and H. Shinohara, Production and isolation of an ellipsoidal C_{80} fullerene, *Chem. Commun.*, 2000, 557–558, DOI: **10.1039/B000387P**.

6 W. Shen, L. Bao, S. Hu, X. Gao, Y. Xie, X. Gao, W. Huang and X. Lu, Isolation and Crystallographic Characterization of $Lu_3N@C_{2n}$, ($2n$ = 80-88): Cage Selection by Cluster Size, *Chem. – Eur. J.*, 2018, **24**, 16692–16698.
7 S. Yang and L. Dunsch, Expanding the Number of Stable Isomeric Structures of the C_{80} Cage: A New Fullerene $Dy_3N@C_{80}$, *Chem. – Eur. J.*, 2006, **12**, 413–419.
8 P. Fowler and D. Manolopoulos, *An Atlas of Fullerenes*, Oxford Press, Clarendon, 1995.
9 M. Guo, X. Li, Y.-R. Yao, J. Zhuang, Q. Meng, Y. Yan, X. Liu and N. Chen, A non-isolated pentagon rule C_{82} cage stabilized by a stretched Sc_3N cluster, *Chem. Commun.*, 2021, **57**, 4150–4153.
10 A. Liu, M. Nie, Y. Hao, Y. Yang, T. Wang, Z. Slanina, H. Cong, L. Feng, C. Wang and F. Uhlik, $Ho_2O@C_{74}$: Ho_2O Cluster Expands within a Small Non-IPR Fullerene Cage of C_s,$_2$(13333)-C_{74}, *Inorg. Chem.*, 2019, **58**, 4774–4781.
11 S. Stevenson, A. J. Rothgeb, K. R. Tepper, J. Duchamp, H. C. Dorn, X. B. Powers, M. Roy, M. M. Olmstead and A. L. Balch, Isolation and Crystallographic Characterization of Two, Nonisolated Pentagon Endohedral Fullerenes: $Ho_3N@C_s$,$_2$(22010)-C_{78} and $Tb_3N@C_2$(22010)-C_{78}, *Chem. – Eur. J.*, 2019, **25**, 12545–12551.
12 N. Chen, C. M. Beavers, M. Mulet-Gas, A. Rodríguez-Fortea, E. J. Munoz, Y. Li, M. M. Olmstead, A. L. Balch, J. M. Poblet and L. Echegoyen, $Sc_2S@C_s$,(10528)-C_{72}: A Dimetallic Sulfide Endohedral Fullerene with a Non Isolated Pentagon Rule Cage, *J. Am. Chem. Soc.*, 2012, **134**, 7851–7860.
13 C. Wang, T. Kai, T. Tomiyama, T. Yoshida, Y. Kobayashi, E. Nishibori, M. Takata, M. Sakata and H. Shinohara, C_{66} fullerene encaging a scandium dimer, *Nature*, 2000, **408**, 426–427.
14 S. Stevenson, P. W. Fowler, T. Heine, J. C. Duchamp, G. Rice, T. Glass, K. Harich, E. Hajdu, R. Bible and H. C. Dorn, A stable non-classical metallofullerene family, *Nature*, 2000, **408**, 427–428.
15 L. Bao, P. Yu, C. Pan, W. Shen and X. Lu, Crystallographic identification of $Eu@C_{2n}$, ($2n$ = 88, 86 and 84): completing a transformation map for existing metallofullerenes, *Chem. Sci.*, 2019, **10**, 2153–2158.
16 J. Zhang, F. L. Bowles, D. W. Bearden, W. K. Ray, T. Fuhrer, Y. Ye, C. Dixon, K. Harich, R. F. Helm, M. M. Olmstead, A. L. Balch and H. C. Dorn, A missing link in the transformation from asymmetric to symmetric metallofullerene cages implies a top-down fullerene formation mechanism, *Nat. Chem.*, 2013, **5**, 880–885.
17 C.-H. Chen, L. Abella, M. R. Cerón, M. A. Guerrero-Ayala, A. Rodríguez-Fortea, M. M. Olmstead, X. B. Powers, A. L. Balch, J. M. Poblet and L. Echegoyen, Zigzag Sc_2C_2 Carbide Cluster inside a [88]Fullerene Cage with One Heptagon, $Sc_2C_2@C_s$(hept)-C_{88}: A Kinetically Trapped Fullerene Formed by C_2 Insertion?, *J. Am. Chem. Soc.*, 2016, **138**, 13030–13037.
18 W. Cai, L. Abella, J. Zhuang, X. Zhang, L. Feng, Y. Wang, R. Morales-Martínez, R. Esper, M. Boero, A. Metta-Magaña, A. Rodríguez-Fortea, J. M. Poblet, L. Echegoyen and N. Chen, Synthesis and Characterization of Non-Isolated-Pentagon-Rule Actinide Endohedral Metallofullerenes $U@C_1$(17418)-C_{76}, $U@C_1$(28324)-C_{80}, and $Th@C_1$(28324)-C_{80}: Low-Symmetry Cage Selection Directed by a Tetravalent Ion, *J. Am. Chem. Soc.*, 2018, **140**, 18039–18050.
19 W. Cai, J. Alvarado, A. Metta-Magaña, N. Chen and L. Echegoyen, Interconversions between Uranium Monometallofullerenes: Mechanistic Implications and Role of Asymmetric Cages, *J. Am. Chem. Soc.*, 2020, **142**, 13112–13119.
20 W. Krätschmer, K. Fostiropoulos and D. R. Huffman, The infrared and ultraviolet absorption spectra of laboratory-produced carbon dust: evidence for the presence of the C_{60} molecule, *Chem. Phys. Lett.*, 1990, **170**, 167–170.
21 Q. Tang, L. Abella, Y. Hao, X. Li, Y. Wan, A. Rodríguez-Fortea, J. M. Poblet, L. Feng and N. Chen, $Sc_2O@C_{2v}(5)$-C_{80}: Dimetallic Oxide Cluster Inside a C_{80} Fullerene Cage, *Inorg. Chem.*, 2015, **54**, 9845–9852.
22 H. Kurihara, X. Lu, Y. Iiduka, N. Mizorogi, Z. Slanina, T. Tsuchiya, T. Akasaka and S. Nagase, $Sc_2C_2@C_{80}$ Rather than $Sc_2@C_{82}$: Templated Formation of Unexpected $C_{2v}(5)$-C_{80} and Temperature-Dependent Dynamic Motion of Internal Sc_2C_2 Cluster, *J. Am. Chem. Soc.*, 2011, **133**, 2382–2385.
23 L. N. Dawe, T. A. AlHujran, H.-A. Tran, J. I. Mercer, E. A. Jackson, L. T. Scott and P. E. Georghiou, Corannulene and its penta-*tert*-butyl derivative co-crystallize 1:1 with pristine C_{60}-fullerene, *Chem. Commun.*, 2012, **48**, 5563–5565.
24 G. Velkos, W. Yang, Y.-R. Yao, S. M. Sudarkova, X. Liu, B. Büchner, S. M. Avdoshenko, N. Chen and A. A. Popov, Shape-adaptive single-molecule magnetism and hysteresis up to 14 K in oxide clusterfullerenes $Dy_2O@C_{72}$ and $Dy_2O@C_{74}$ with fused pentagon pairs and flexible Dy–(μ_2-O)–Dy angle, *Chem. Sci.*, 2020, **11**, 4766–4772.
25 Y. Hao, L. Feng, W. Xu, Z. Gu, Z. Hu, Z. Shi, Z. Slanina and F. Uhlík, $Sm@C_{2v}$(19138)-C_{76}: A Non-IPR Cage Stabilized by a Divalent Metal Ion, *Inorg. Chem.*, 2015, **54**, 4243–4248.
26 C. M. Beavers, M. N. Chaur, M. M. Olmstead, L. Echegoyen and A. L. Balch, Large Metal Ions in a Relatively Small Fullerene Cage: The Structure of $Gd_3N@C_s$,$_2$(22010)-C_{78} Departs from the Isolated Pentagon Rule, *J. Am. Chem. Soc.*, 2009, **131**, 11519–11524.
27 A. J. Stone and D. J. Wales, Theoretical studies of icosahedral C_{60} and some related species, *Chem. Phys. Lett.*, 1986, **128**, 501–503.
28 D. J. Wales, M. A. Miller and T. R. Walsh, Archetypal energy landscapes, *Nature*, 1998, **394**, 758–760.
29 W. Cai, C.-H. Chen, N. Chen and L. Echegoyen, Fullerenes as Nanocontainers That Stabilize Unique Actinide Species Inside: Structures, Formation, and Reactivity, *Acc. Chem. Res.*, 2019, **52**, 1824–1833.
30 P. Zhao, M. Li, Y.-J. Guo, R. Zhao and X. Zhao, Single Step Stone-Wales Transformation Linking Two Thermodynamically Stable $Sc_2O@C_{78}$ Isomers, *Inorg. Chem.*, 2016, **55**, 2220–2226.

31 Y. Hao, Q. Tang, X. Li, M. Zhang, Y. Wan, L. Feng, N. Chen, Z. Slanina, L. Adamowicz and F. Uhlík, Isomeric $Sc_2O@C_{78}$ Related by a Single-Step Stone-Wales Transformation: Key Links in an Unprecedented Fullerene Formation Pathway, *Inorg. Chem.*, 2016, **55**, 11354–11361.
32 G. Sheldrick, A short history of SHELX, *Acta Crystallogr., Sect. A: Found. Crystallogr.*, 2008, **64**, 112–122.
33 M. Ernzerhof and G. E. Scuseria, Assessment of the Perdew–Burke–Ernzerhof exchange-correlation functional, *J. Chem. Phys.*, 1999, **110**, 5029–5036.
34 W. J. Hehre, R. Ditchfield and J. A. Pople, Self—Consistent Molecular Orbital Methods. XII. Further Extensions of Gaussian—Type Basis Sets for Use in Molecular Orbital Studies of Organic Molecules, *J. Chem. Phys.*, 1972, **56**, 2257–2261.
35 P. C. Hariharan and J. A. Pople, The influence of polarization functions on molecular orbital hydrogenation energies, *Theor. Chim. Acta*, 1973, **28**, 213–222.
36 M. Dolg, H. Stoll and H. Preuss, A combination of quasirelativistic pseudopotential and ligand field calculations for lanthanoid compounds, *Theor. Chim. Acta*, 1993, **85**, 441–450.
37 K. Zhang, H. Zheng, M. Li, Q. Li, Y. Zhao and X. Zhao, Significant Roles of a Particularly Stable Two-Center Two-Electron Lu–Lu σ Bond in $Lu_2@C_{86}$: Electronic Structure of Lu and Radius of Lu^{2+}, *Inorg. Chem.*, 2021, **60**, 2425–2436.
38 R. Krishnan, J. S. Binkley, R. Seeger and J. A. Pople, Self–consistent molecular orbital methods. XX. A basis set for correlated wave functions, *J. Chem. Phys.*, 1980, **72**, 650–654.
39 X. Cao and M. Dolg, Valence basis sets for relativistic energy-consistent small-core lanthanide pseudopotentials, *J. Chem. Phys.*, 2001, **115**, 7348–7355.
40 R. Gulde, P. Pollak and F. Weigend, Error-Balanced Segmented Contracted Basis Sets of Double-ζ to Quadruple-ζ Valence Quality for the Lanthanides, *J. Chem. Theory Comput.*, 2012, **8**, 4062–4068.
41 B. P. Pritchard, D. Altarawy, B. Didier, T. D. Gibson and T. L. Windus, New Basis Set Exchange: An Open, Up-to-Date Resource for the Molecular Sciences Community, *J. Chem. Inf. Model.*, 2019, **59**, 4814–4820.
42 M. J. Frisch, G. W. Trucks, H. B. Schlegel, G. E. Scuseria, M. A. Robb, J. R. Cheeseman, G. Scalmani, V. Barone, G. A. Petersson, H. Nakatsuji, X. Li, M. Caricato, A. V. Marenich, J. Bloino, B. G. Janesko, R. Gomperts, B. Mennucci, H. P. Hratchian, J. V. Ortiz, A. F. Izmaylov, J. L. Sonnenberg, D. Williams-Young, F. Ding, F. Lipparini, F. Egidi, J. Goings, B. Peng, A. Petrone, T. Henderson, D. Ranasinghe, V. G. Zakrzewski, J. Gao, N. Rega, G. Zheng, W. Liang, M. Hada, M. Ehara, K. Toyota, R. Fukuda, J. Hasegawa, M. Ishida, T. Nakajima, Y. Honda, O. Kitao, H. Nakai, T. Vreven, K. Throssell, J. A. Montgomery Jr., J. E. Peralta, F. Ogliaro, M. J. Bearpark, J. J. Heyd, E. N. Brothers, K. N. Kudin, V. N. Staroverov, T. A. Keith, R. Kobayashi, J. Normand, K. Raghavachari, A. P. Rendell, J. C. Burant, S. S. Iyengar, J. Tomasi, M. Cossi, J. M. Millam, M. Klene, C. Adamo, R. Cammi, J. W. Ochterski, R. L. Martin, K. Morokuma, O. Farkas, J. B. Foresman and D. J. Fox, *Gaussian 16, Revision A.03*, Gaussian, Inc., Wallingford CT, 2016.

